A Bidirectional Lens-Free Digital-Bits-In/-Out 0.57mm^2 Terahertz Nano-Radio in CMOS with 49.3mW Peak Power Consumption Supporting 50cm Internet-of-Things Communication

Taiyun Chi[1], Hechen Wang[2], Min-Yu Huang[1], Fa Foster Dai[2], and Hua Wang[1]
1. School of Electrical and Computer Engineering, Georgia Tech, Atlanta, GA 30332 USA
2. Dept. of Electrical and Computer Engineering, Auburn University, Auburn, AL 36849 USA

***Abstract*—A CMOS digital-bits-in/-out Terahertz (THz) nano-radio with 0.57mm^2 chip area is presented in this paper. The THz operation and bidirectional transmitter/receiver (TX/RX) architecture lead to radio ultra-miniaturization for Internet-of-Things (IoT) and field-deployable sensor applications. The bidirectional THz radio is configured as a harmonic oscillator in the TX mode or as a super-harmonic super-regenerative RX in the RX mode. The TX harmonic oscillator is directly modulated by On-Off Keying (OOK) data for bits-to-THz transmitting, while an on-chip time-to-digital converter (TDC) with 25ps timing resolution measures RX oscillation start-up time for direct THz-to-bits receiving. The radio peak DC power is optimized based on link distance and data rate. It supports maximum 4.4Mb/s OOK over 50cm at 49.3mW peak DC power and 1Mb/s OOK over 17cm at 18.7mW peak DC power without using any Silicon lens.**

***Keywords*—bidirectional, CMOS integrated circuits, Internet of Things, on-chip antennas, radio transceivers, terahertz (THz).**

I. Introduction

There is an increasing need for highly integrated radio systems to address field-deployable and massively-producible applications in future commercial markets, such as wireless sensor networks, medical implants, and Internet-of-Things (IoT) devices. These applications place stringent requirements on the radio solutions which need to offer an ultra-compact form-factor (<1mm^3), a low peak DC power consumption (<50mW), a sufficient communication distance (>0.5m), and a useful data rate (>1Mb/s). Many integrated radio systems, however, cannot satisfy such demanding SWaP (Size-Weight-and-Power) requirements. A major challenge lies in the physical size of a radio that is often dominated by its antenna. Conventional GHz low-power radios [1] or mm-wave radios [2] require cm-/mm-sized antennas, limiting the radio miniaturization. The continuous device scaling allows for THz Silicon-based radios with drastic antenna size reduction and sub-mm-sized form-factor [3]–[5]. However, most existing THz radios consume a large DC power (P_{DC}) [3]–[5] and are thus incompatible with field-deployable applications.

In order to bridge this unmet technology gap, a digital-bits-in/-out CMOS THz nano-radio is proposed in this paper (Fig. 1). The antenna size at THz is substantially reduced to enable ultra-miniaturized radios. A bidirectional transmitter/receiver (TX/RX) circuit-sharing architecture configures the radio as a harmonic oscillator in the TX mode or as a super-harmonic super-regenerative receiver in the RX mode. The super-regenerative RX offers high sensitivity to compensate the THz path loss. A THz on-chip antenna is shared by the TX/RX for further radio size reduction. The TX is directly driven by On-Off Keying (OOK) digital data, while an on-chip time-to-digital converter (TDC) provides digitized RX outputs. The proposed THz nano-radio is capable of bidirectional communication of 1Mb/s OOK signal (BER<10^{-7}) with a 50cm communication distance at 26.4mW P_{DC}, and P_{DC} increases to 49.7mW to achieve a maximum data rate of 4.4Mb/s.

This paper is organized as follows. Section II presents the design details of the proposed bidirectional THz nano-radio. The measurement results are summarized in Section III. Section IV concludes this paper with a comparison table.

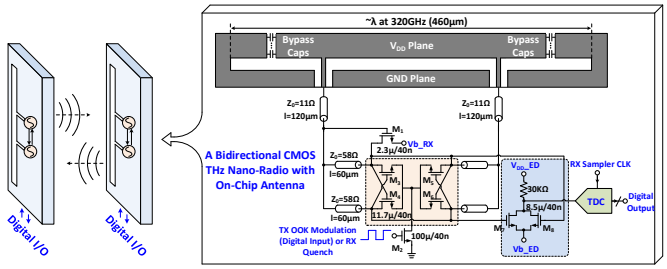

Fig. 1. A bidirectional lens-free digital-bits-in/-out CMOS THz nano-radio with on-chip antenna for Internet-of-Things (IoT) applications.

II. Bidirecional THz Nano-Radio Implementaiton

A. TX Mode

In the TX mode, two coupled oscillators at f_0=160GHz generate a 2nd harmonic signal ($2f_0$=320GHz) as the THz output (Fig. 2). Cross-coupled transistors M_3–M_6 provide differential negative g_m for oscillation. The drain transmission lines (T-lines) TL_3–TL_6 and the device parasitic capacitors form the resonator tank at f_0=160GHz. The T-lines further perform impedance matching to the on-chip slot antenna at $2f_0$ to maximize the output power (P_{out}), and the two in-phase $2f_0$ currents are power-combined on the antenna. Transistors M_7 and M_8 are used as varactors for frequency tuning. The OOK signal directly drives the tail current source M_2 for bits-to-THz transmitting. The TX P_{out} can be backed-off by lowering the tail bias current and reducing the TX P_{DC} for short link distances. The TDC and the RX injection transistor M_1 are turned off in the TX mode.

978-1-5090-5191-5/17/$31.00@2017 IEEE

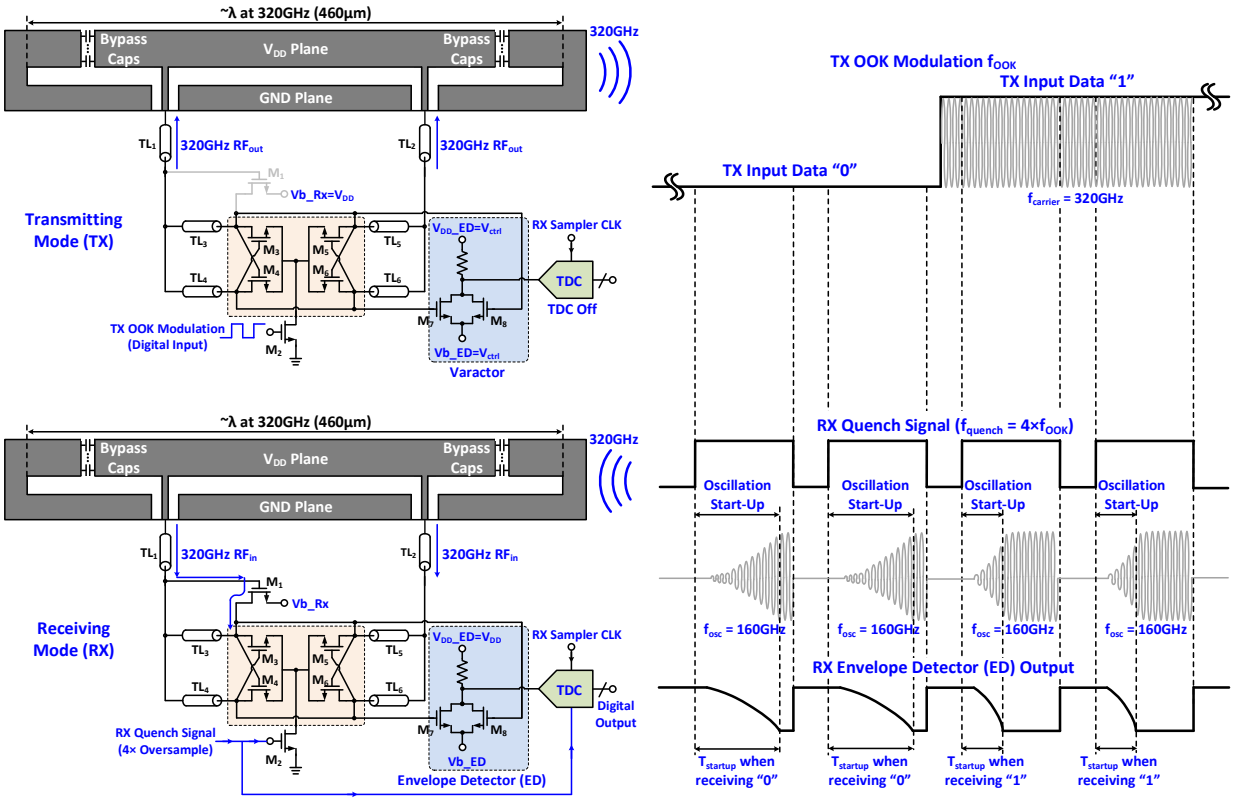

Fig. 2. Circuit schematic of the THz nano-radio configured as the transmitting mode (TX) and the receiving mode (RX).

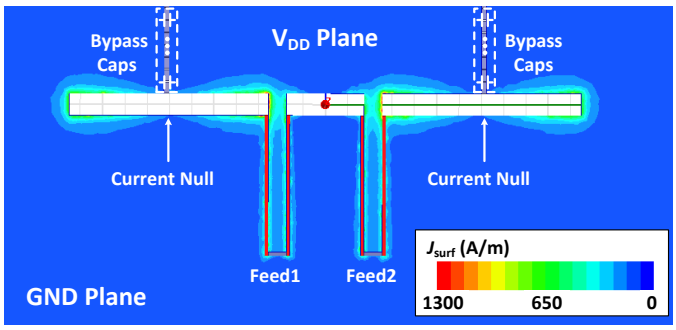

Fig. 3. 3D EM-simulated surface current distribution (J_{surf}) of the on-chip two-feed slot antenna at 320GHz.

An on-chip antenna is integrated to achieve THz radiation and receiving. It is shared between the TX and RX mode radio operations for area saving. A two-feed slot antenna [6] is implemented, which consists of a V_{DD} plane and a GND plane (Fig. 3). The V_{DD} plane is DC-connected to the drain nodes of the cross-coupled M_3–M_6 for supply feeding. Sufficient bypass capacitors are needed to decouple the V_{DD} plane from the GND plane. However, on-chip MOM capacitors exhibit poor quality factor (Q) at THz range, leading to severe signal loss of the THz radiation signal and radiation efficiency degradation, especially at low antenna driving impedance (~11Ω in this design). To minimize the loss from the bypass capacitors, the slot antenna is designed with a total length around λ, so that it presents two current nulls on the antenna. The 3D EM-simulated current distribution of the two-feed slot antenna at 320GHz is shown in Fig. 3. The V_{DD} plane and the GND plane are then separated and bypassed at these two antenna current nulls using MOM capacitors, ensuring minimal signal loss.

B. RX Mode

In the RX mode, the radio is reconfigured as a super-harmonic super-regenerative RX to detect the incoming OOK-modulated THz signal at $2f_0$ (Fig. 2). Once a $2f_0$ input signal is received by the on-chip antenna, M_1 injects a $2f_0$ current into the resonator tank and creates a small asymmetry to perturb the fundamental oscillation start-up at f_0. Thus, the received OOK signal leads to different RX oscillation start-up time (Fig. 2). Transistors M_7 and M_8 are reconfigured as an envelope detector (ED) whose output triggers the TDC. By periodically quench the tail current source M_2 with 4× oversampling, OOK demodulation is realized by the digitized oscillation start-up time from the TDC, achieving direct THz-to-bits receiving. This super-harmonic super-regenerative RX substantially improves the RX sensitivity over non-coherent THz power-detector RX, and it exhibits competitive sensitivity but at significantly lower P_{DC} compared with coherent down-conversion RX beyond transistor f_{max}.

A fine TDC timing resolution and a large detectable timing range are needed to resolve the RX oscillation start-up time. The TDC comprises a sampler as a coarse TDC and a fine TDC with a 2D Vernier structure [7] (Fig. 4). The coarse TDC resolution is 500ps, while the fine TDC comprises two slightly differed delay lines and a 2D comparator array, covering 725ps range at a resolution of 25ps. Once the RX quench signal turns on the THz oscillator, its start-up time is first sampled by the

coarse TDC until the ED output triggers the fine TDC whose output resolves the coarse TDC residue (Fig. 4). The RX oscillation start-up time is thus the output difference of the coarse and fine TDCs. The TDC only consumes 0.7mW including CLK buffers. At low data rate, the duty cycle of the quench signal is reduced to save RX P_{DC}.

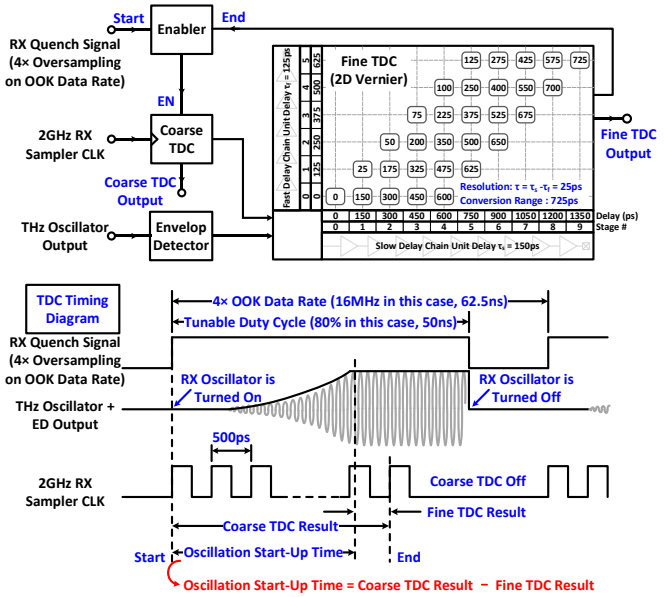

Fig. 4. Circuit schematic of the TDC, and the TDC timing diagram.

III. Measurement Results

The bidirectional THz nano-radio is implemented in a 45nm CMOS SOI process with a high-resistivity substrate (Fig. 5). The miniaturized THz TRX only occupies 0.95×0.6mm^2 including all the pads. The CMOS chip is wire-bonded to a PCB to facilitate the testing.

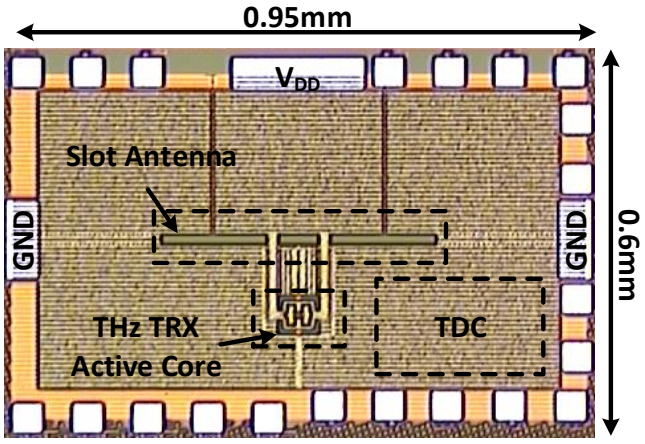

Fig. 5. Chip microphtograph of the bidirectional THz nano-radio.

The TX mode of the THz nano-radio is characterized first. Figure 6 shows the measurement setup together with the measured frequency tuning, EIRP versus P_{DC}, and calculated DC-to-EIRP efficiency. Three TX chips are measured, and the maximum frequency difference is only 1.2GHz, verifying the design robustness. The nano-radio frequency is tunable from 316 to 321GHz. The measured TX peak EIRP is -11.6dBm with a peak 0.19% DC-to-EIRP efficiency at 36.3mW TX P_{DC}.

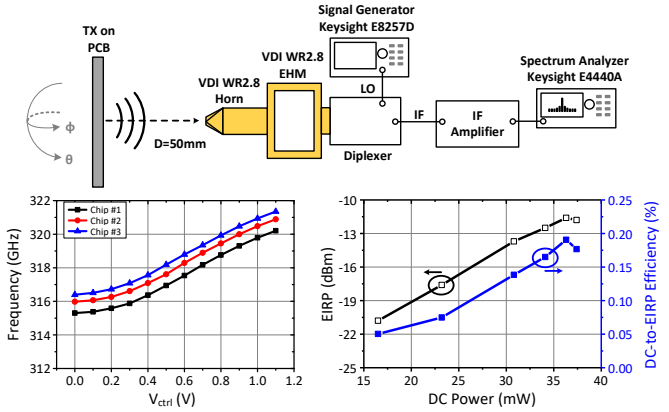

Fig. 6. Continuous-wave (CW) measurement setup in the TX mode, measured TX frequency tuning ranges for three independent samples, measured TX EIRP vs. DC power consumption (P_{DC}), and calculated DC-to-EIRP efficiency.

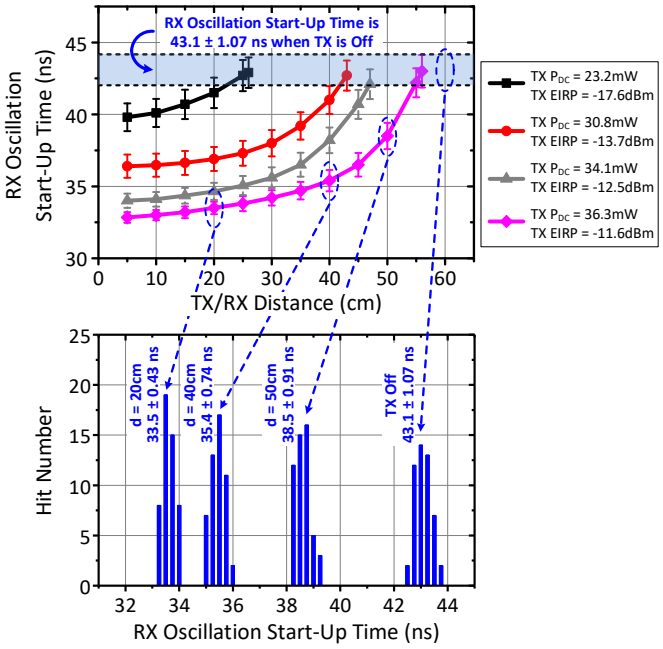

Fig. 7. THz nano-radio communication link CW characterization, including measured RX oscillation start-up time vs. TX/RX communication distance at different TX P_{DC}, and typical RX start-up timing histograms at 36.3mW TX P_{DC} with 50 measurement results collected for each communication distance.

Next, two THz nano-radio chips are used as TX/RX to establish and characterize the THz wireless link.

In the continuous-wave (CW) link measurements, the RX oscillation start-up time is measured against the TX/RX communication distance and TX EIRP set by TX P_{DC} (Fig. 7). At each TX/RX distance and TX power setting, 50 measurements are collected to compute the mean and standard deviation of the RX oscillation start-up time. When the TX is off, the RX oscillation start-up time is measured as

43.1±1.07ns. For a given TX P_{DC}, the RX oscillation start-up time increases for larger TX/RX distances due to the reduced receiving THz power. For a fixed TX/RX distance, the RX oscillation start-up time increases when TX power is reduced. The maximum CW communication distance is 55cm at 36.3mW TX P_{DC}. The RX sensitivity is extracted as -89dBm using the measured TX EIRP and the path loss. Typical RX start-up timing histograms are shown in Fig. 7.

Finally, OOK communication is established between the two THz nano-radio chips. The measured data rate, TX/RX distance, and TRX total P_{DC} are shown in Fig. 8. The maximum data rate of 4.4Mb/s (BER<10^{-7}) over 50cm maximum TX/RX distance is supported at a peak 49.3mW TRX P_{DC}. The total TRX P_{DC} can be optimized based on the actual link distance and data rate (Fig. 8). This is achieved by lowering the TX P_{out} for closer communication distances and reducing the RX quench signal duty cycle at lower data rates. For example, the TRX only consumes 18.7mW P_{DC} to maintain 1Mb/s OOK over 17cm. The BER and minimum RX P_{DC} versus data rate over 50cm as well as BER versus distance at different TX P_{DC} for 4Mb/s OOK are also shown in Fig. 8.

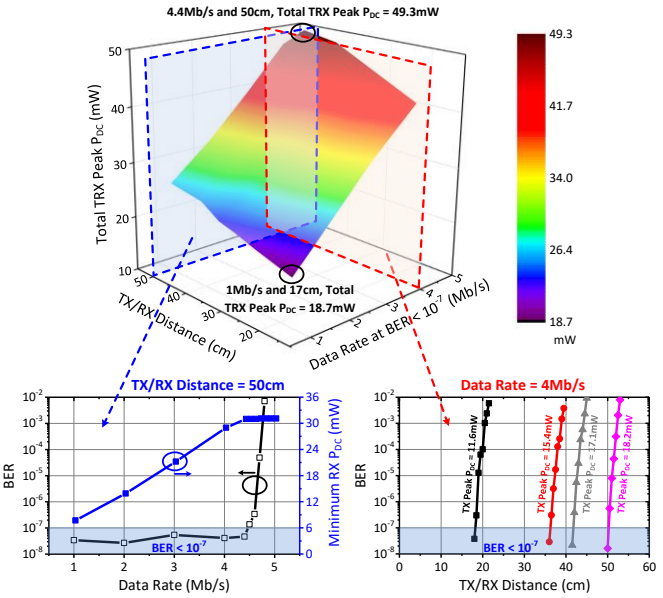

Fig. 8. THz nano-radio communication link using OOK modulations. The results are summarized as measured TRX peak P_{DC} versus different TX/RX communication distances and OOK data rates at BER<10^{-7}.

IV. Conclusions

A CMOS THz nano-radio is proposed and demonstrated in this paper that achieves drastic radio miniaturization for IoT and field-deployable sensor applications. The bidirectional circuit sharing architecture configures the THz nano-radio as an OOK-modulated harmonic oscillator in the TX mode or as a super-harmonic super-regenerative RX that offers high sensitivity at significantly reduced DC power than coherent down-conversion RX. A TDC is integrated on-chip to directly achieve digitalized outputs in the RX mode with only 0.7mW P_{DC}, minimizing any post analog signal processing.

Compared with the reported Silicon-based 300GHz TRXs, this bidirectional THz nano-radio achieves the lowest P_{DC} (49.7mW) and the longest communication distance (50cm) without any Silicon lens (TABLE I). It also achieves the highest radio miniaturization (>7.8× radio size reduction), competitive data rate (maximum 4.4Mb/s with BER<10^{-7}), and P_{DC} compared with GHz/mm-wave low-power radios (TABLE I). The reported power consumption is the peak P_{DC} during the radio operation. Heavily duty-cycled operations, typical for sensor nodes and IoT devices, will substantially reduce the THz nano-radio averaged P_{DC} down to µW level.

TABLE I
Comparison with State-of-the-Art THz Tranceivers and GHz/mm-Wave Low-Power Radios

	This Work	[3]	[4]	[5]	[1]	[2]
Frequency (GHz)	**320**	380	240	210	0.112 (TX), 0.05 (RX)	60 (TX), 24(RX)
Radio Size (mm^2)	**0.57 (TRX)**	4.18 (TRX)	1.70 (TX)	3.5 (TX)	2.22 (TRX)	4.44 (TRX)
			1.57 (RX)	1.12 (RX)	8 (Antenna)	
TX EIRP (dBm)	**-11.6**	-13	21.9 (Si Lens)	5.1	N/A (Near-Field Radio)	-6.5
RX Sensitivity (dBm)	**-89**	-40†	-60†	-64†	-54 at 100kps	-10.5
Peak DC Power (mW)	**18.2 (TX)***	364 (TRX)	1033 (TX)	240 (TX)	13.6 (TX)	N/A
	31.1 (RX)*		886 (RX)	68 (RX)	0.036 (RX)	
Max. Communication Distance (cm)	**50**	10	15	3.5	50 (TX)	50
					20 (RX)	
Data Rate, Modulation Type, BER	**4.4Mb/s OOK, 10^{-7}**	Chirp	2.73Gb/s QPSK, 10^{-9}	CW	2kb/s OOK, 10^{-3}	12Mb/s M-PPM, 10^{-3}
Technology	**45nm CMOS SOI**	130nm SiGe	130nm SiGe	32nm CMOS SOI	180nm CMOS	65nm CMOS

* TX peak P_{DC} assumes 50% duty-cycle OOK. RX peak P_{DC} includes the on-chip TDC DC power of 0.7mW.
† Defined as Sensitivity = -174dBm/Hz + 10logBW + NF with BW = 8GHz. In this work, a 50% change in the RX oscillation start-up time difference from 316 to 324GHz is mesaured to define the RX RF BW [8].

Acknowledgment

This work was supported by the US Army Research Office under Grant No. W911NF-15-P-0021. The authors would like to thank GlobalFoundries for chip fabrication. We also thank members in GT GEMS Lab for helpful technical discussions.

References

[1] Y. Shi, *et al.*, "A 10mm^3 syringe-implantable near-field radio system on glass substrate", *ISSCC Dig. Tech. Papers*, pp. 448–449, Feb. 2016.

[2] M. Tabesh, N. Dolatsha, A. Arbabian, and A. Niknejad, "A power-harvesting pad-less millimeter-sized radio", *IEEE J. Solid-State Circuits*, vol. 50, no. 4, pp. 962–977, Apr. 2015.

[3] J. Park, S. Kang, and A. Niknejad, "A 0.38 THz fully integrated transceiver utilizing a quadrature push-push harmonic circuitry in SiGe BiCMOS," *IEEE Symp. VLSI Circuits*, pp. 22–23, June 2011.

[4] N. Sarmah, *et al.*, "A fully integrated 240-GHz direct-conversion quadrature transmitter and receiver chipset in SiGe technology," *IEEE Trans. Microw. Theory Techn.*, vol. 64, no. 2, pp. 562–574, Feb. 2016.

[5] Z. Wang, *et al.*, "A 210 GHz fully integrated differential transceiver with fundamental-frequency VCO in 32 nm SOI CMOS," *ISSCC Dig. Tech. Papers*, pp. 136–137, Feb. 2013.

[6] S. Li, T. Chi, J. Park, and H. Wang, "A multi-feed antenna for antenna-level power combining," in *Proc. IEEE APS/URSI Symp.*, June 2016.

[7] J. Yu, F. Dai, and R. Jaeger, "A 12-bit vernier ring time-to-digital converter in 0.13µm CMOS technology," in *Proc. IEEE Symp. VLSI Circuits*, pp. 232–233, June 2009.

[8] A. Tang and M.-C. Chang, "183GHz 13.5mW/pixel CMOS regenerative receiver for mm-wave imaging applications," *ISSCC Dig. Tech. Papers*, pp. 296–297, Feb. 2011.